Research Square

Preprints are preliminary reports that have not undergone peer review.
They should not be considered conclusive, used to inform clinical practice,
or referenced by the media as validated information.

Time-series insights of the geomorphologic changes of the Hunga submarine caldera

Marta Ribó

marta.ribo.gene@aut.ac.nz

Auckland University of Technology https://orcid.org/0000-0002-6211-7007

Shane Cronin

University Auckland https://orcid.org/0000-0001-7499-603X

James Garvin

Goddard Space Flight Center https://orcid.org/0000-0003-1606-5645

Isobel Yeo

National Oceanography Centre

Michael Clare

National Oceanography Centre https://orcid.org/0000-0003-1448-3878

Sally Watson

National Institute of Water and Atmospheric Research https://orcid.org/0000-0002-3666-5034

Gerd Sielfeld

University of Auckland

James Hunt

National Oceanography Centre https://orcid.org/0000-0001-9852-6200

Daniel Slayback

NASA Goddard Space Flight Center

Sung-Hyun Park

Korea Polar Research Institute https://orcid.org/0000-0002-6303-4879

Briony Hutton

Echoview Software

Sönke Stern

University of Auckland

James White

University of Otago https://orcid.org/0000-0002-2970-711X

Marco Brenna

Otago University https://orcid.org/0000-0001-6096-6999

Kevin Mackay

NIWA https://orcid.org/0000-0002-1380-7263

Mele Manu

Tonga Geological Service. Ministry of Lands, Surveys, Planning and Natural Resources

Folauhola Latu'ila
Ministry of Natural Resources

Nikolasi Heni
Tonga Geological Service. Ministry of Lands, Surveys, Planning and Natural Resources

Pupunu Tuku’afu
Tonga Geological Service. Ministry of Lands, Surveys, Planning and Natural Resources

Taaniela Kula
Ministry of Natural Resources

Article

Keywords:

Posted Date: October 15th, 2025

DOI: https://doi.org/10.21203/rs.3.rs-7736926/v1

License: This work is licensed under a Creative Commons Attribution 4.0 International License.
Read Full License

Additional Declarations: There is **NO** Competing Interest.

Version of Record: A version of this preprint was published at Nature Geoscience on September 11th, 2026. See the published version at https://doi.org/10.1038/s41561-026-02099-7.

Time-series insights of the geomorphologic changes of the Hunga submarine caldera

Ribó, M[1], Cronin, S.J.[2], Garvin, J.[3], Yeo, I.A.[4], Clare, M. A.[4], Watson, S.J.[5,6], Sielfeld, G.[2], Hunt, J. [4], Slayback, D.[3], Park, S-H.[7], Briony Hutton[8], Stern, S.[2],White, J.D.L.[9], Brenna, M.[9], Mackay, K.[5], Manu, M. S. [10], Latu'ila, F.[10], Heni, N.[10], Tuku'afu, P.[10], Kula, T.[10].

[1]School of Science, Auckland University of Technology, Auckland, Aotearoa New Zealand
[2]School of Environment, The University of Auckland, Auckland, Aotearoa New Zealand
[3]NASA Goddard Space Flight Center, Greenbelt, MD, USA
[4]National Oceanography Centre, Southampton, United Kingdom
[5]Earth Science New Zealand, Wellington, Aotearoa New Zealand
[6]Institute of Marine Sciences, University of Auckland, Auckland, Aotearoa New Zealand
[7] Korean Polar Research Institute, Incheon, Republic of South Korea
[8]Echoview Software Pty Ltd, Hobart, Tasmania, Australia
[9]Department of Geology, University of Otago, Dunedin, Aotearoa New Zealand
[10]Tonga Geological Service, Natural Resources Division, Ministry of Lands, Surveys, Planning and Natural Resources, Nuku'alofa, Tonga

Abstract

Caldera volcanoes produce the most impactful eruptions worldwide, yet caldera formation is rarely observed, especially in the submarine environment. We report repeat high-resolution seafloor mapping and quantify the geomorphological changes after the 15 January 2022 eruption of Hunga volcano (Tonga). While the ~1800 m-high stratovolcano retained its overall form, islands, shoals and the shallow caldera floor (~150-200 m water depth) collapsed, forming a ~3.5 km diameter basin, ~850 m deep, with its structural floor ~100-150 m below. The total displaced volume is 8.9 ± 0.1 km³. Of this, 6.85 ± 0.05 km³ is attributed to caldera collapse, reflecting loss of magma from the ~2–6 km deep reservoir; and ~2 km³ was removed by erosion from eruption-fed density currents and undercutting of the southern edifice flanks.

Caldera morphology suggests multiple episodes of trapdoor and piston subsidence, while inner-caldera landslide deposits intercalated with pyroclastic infill indicates caldera collapse was syn-eruptive. Observed fluid vents in May 2022 highlighted two vent zones,

below the collapsed 2014-2015 tephra cone in the NW, and at the SE edge of the caldera basin. These results provide new insights into the mechanisms and geomorphic evolution of highly hazardous mafic caldera eruptions.

Submarine eruptions dominate volcanism on Earth, with submerged and island-volcano calderas associated with some of the largest and deadliest eruptions known[1, 2]. The 1883 eruption of Krakatau, Indonesia, took >30,000 lives and caused widespread devastation with a combination of pyroclastic density currents and tsunami[3]. The 15 January 2022 Hunga eruption produced tsunami of similar size, but fortunately few lives were lost[4]. Despite the recognised threat of submarine caldera volcanoes, most remain poorly characterised due to the challenges and costs associated with acquiring direct field observations in deep marine and remote settings. Detailed insights into eruption-induced geomorphic changes at subaerial volcanoes[5, 6, 7], are replicated by very few repeat bathymetric surveys of submarine volcanoes and usually only in association with minor activity[8, 9, 10]. Most submarine caldera volcanoes remain unmapped or are surveyed at only coarse spatial scales. Without high-resolution bathymetric datasets before and after caldera eruptions, fundamental open questions remain about *i)* the mode(s) of caldera collapse, *ii)* the magnitude of seabed changes within and outside the caldera, and *iii)* the relationship of geomorphic features to the dynamics of volcano-tectonic processes. *In-situ* observations are critical to advancing numerical and analogue modelling of caldera collapse processes, understanding their related landforms[11] and forecasting hazards, including tsunamis[12].

The 2022 Hunga eruption was one the most explosive of the last Century[13, 14, 15]. This shallow submarine eruption had diverse and globally significant impacts, triggering deadly volcanic tsunamis[4, 14], global atmospheric pressure waves[15], and a >55 km-high plume that injected large quantities of volatilised seawater into the atmosphere and stratosphere[16, 17, 18, 19].

During 11 hours, the eruption involved intense explosive magma-seawater interaction[18]. Pre- and post-eruption seafloor surveys in the areas surrounding Hunga volcano revealed deep (>100 m) scours carved into the submerged volcano flanks, and volcanoclastic density currents deposits that caused widespread loss of seafloor life and damaged >190 km of critical submarine telecommunication cables[20, 21].

We analysed the summit plateau of Hunga volcano using a time series of high-resolution bathymetric surveys and water column observations, to relate geomorphologic changes to the dynamics of this major explosive eruption. Comparing bathymetric datasets from 2015, 2016 and 2021 to those from April, May, July and October 2022, we quantify the geomorphologic changes and use this to interpret *i)* magma volume erupted; *ii)* caldera collapse mechanisms; *iii)* depositional and erosional processes; *iv)* caldera-basin water structure and features; and *v)* implications of these findings for hazard evaluations at mafic caldera systems worldwide.

Results

Structural influence on Hunga volcano caldera

Submarine and island caldera volcanoes are numerous along volcanic arcs worldwide[22, 23, 24, 25, 26]. At least 74 submarine volcanoes occur along the Tonga-Kermadec Arc, with Hunga located within the central portion of the Tonga volcanic arc (Fig. 1A). Hunga lies within a zone of weak extension ~190 km ESE of the Tonga Trench axis, ~30 km west of the uplifted arc front, and east of the Lau Basin spreading centre (Fig. 1A). With ~200 mm/yr of convergence, this is the fastest subduction zone[27, 28, 29]. The wider volcanic arc is NNE-SSW orientated, parallel to the subduction zone (Fig. 1B). The pre-2022 bathymetric map near Hunga exposes structural ridges connecting the Hunga caldera to a deeper caldera-like structure ~10 km to the SE (Fig. 1C). This may reflect a weak local extensional structure. The ridge orientation is 45º offset from the Tonga trench and may reflect adjustment of vertical and horizontal stresses

86 induced in the overriding Indo-Australian Plate as the Pacific plate subducts slightly obliquely
87 below (Fig. 1B). The NW-SE local structural feature may influence Hunga structure, as well
88 as the orientation of magma pathways and resulting eruptive vent positions (Fig. 2C).
89 Hunga volcano is a ~1.8 km-high mainly submarine basaltic-andesite to andesite
90 stratovolcano. The emergent parts of Hunga volcano (prior to the 2022 eruption) were two ~2
91 km-long and up to 140 m-high islands located on the NW (Hunga Ha'apai island) and NE
92 (Hunga Tonga island) margins of a broad summit region (Extended Data Fig. 1). These islands
93 expose a succession of outward dipping pyroclastic sequences [2]. Radiocarbon dating of a
94 pyroclastic deposits sequence, and geochemically correlated downwind tephra, suggest that at
95 least one caldera-forming eruption occurred at Hunga around AD1100, with older distal fall
96 deposits suggesting cyclical repetition of this activity [2]. Shallow explosive (Surtseyan)
97 submarine and surface eruptions occurred at Hunga in 1912, 1937 [30], 1988 [31, 32], 2009 [33, 34], and
98 2014-2015 [35]. The 2014-2015 eruption built a 2-km diameter tephra cone that joined the two
99 pre-existing islands of Hunga Ha'apai and Hunga Tonga [35, 36] (Fig. 1C). Nearby island
100 volcanoes (Tofua [37]) and shallow submarine volcanoes (Fonuafo'ou) show similar overall
101 form, composition and caldera size to Hunga. These and other emergent basaltic-andesitic
102 cones (e.g., Kao) are thought to also be potential precursors to calderas.
103

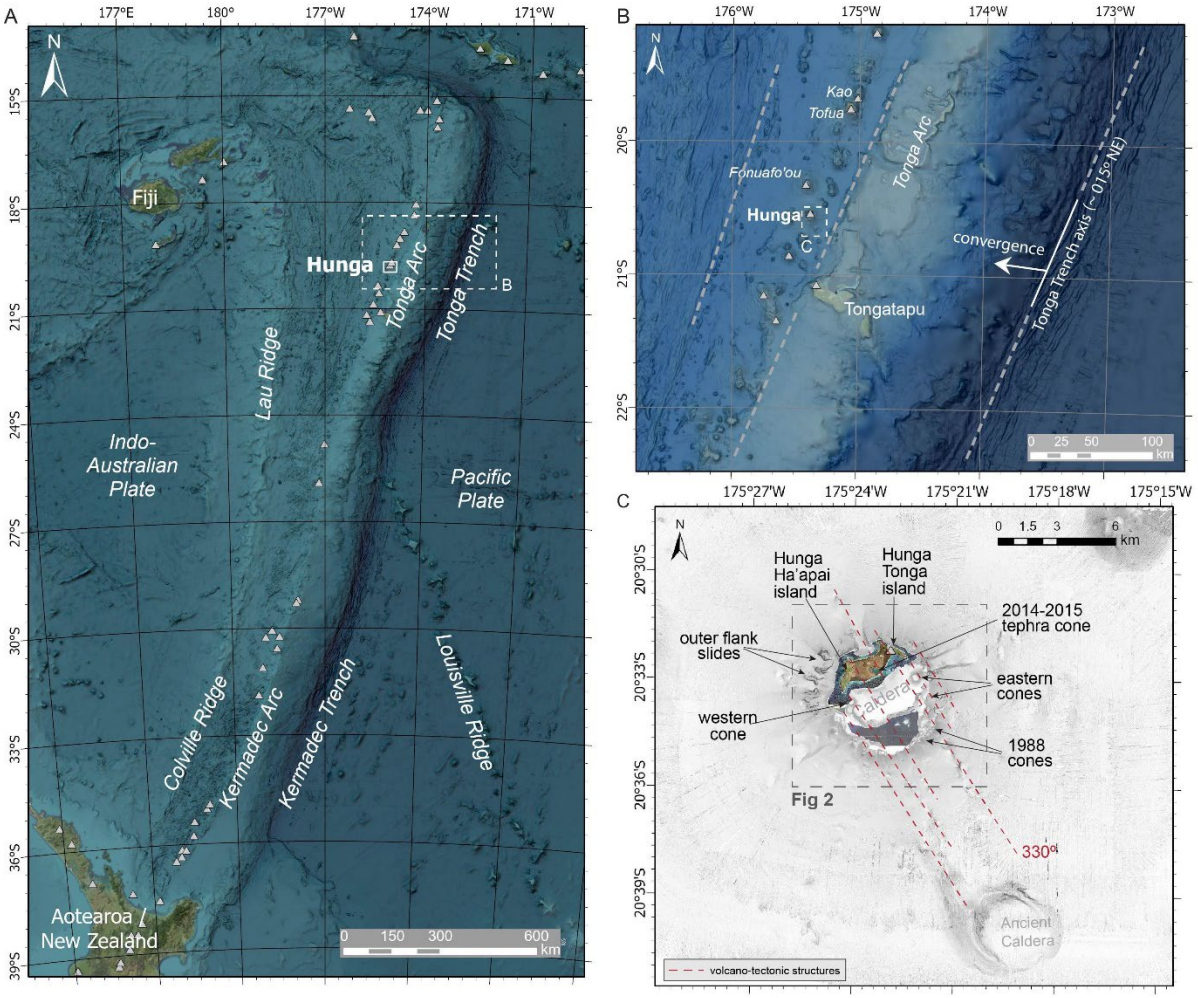


Figure 1. (A) Location map of the Tonga-Kermadec Arc, with the subducting Pacific plate to the east and the northward-widening back-arc Lau basin on the Indo-Australian plate to the west. Light grey triangles indicate the major submarine volcanoes along the Kermadec and Tonga Arcs. White dashed line box indicates area of panel B. **(B)** Location map of Hunga volcano, 65 km north of the main population centre on Tongatapu island. The Tonga Trench axis is orientated ~15º NE, with convergence in this area <5º from perpendicular. White dashed line box indicates the location of panel C. **(C)** pre-2022 bathymetric map of the area of Hunga volcano, with interpreted local volcano-tectonic structures (red dashed lines). Black dashed line box indicates the area shown in Figure 2.

Caldera morphology and volume changes

The pre-eruption Hunga volcano had a ~5.6 km-diameter edifice, which included the two long-lived islands of Hunga Ha'apai and Hunga Tonga, and the 2014-15 tephra cone (Fig. 2). More than ~22 cones are located around the outer circumference of the summit, marking the presence of a long-lived caldera. These cones commonly have crater-features and outer flank diameters between ~100 and 160 m, with exceptions of one of ~200 m diameter in the west,

and another of 700 m diameter in the east (Fig. 2A). The central part of Hunga summit caldera contained a ~2 x 4 km WSW-ENE oriented basin with water depths between 150-200 m (Fig. 2A). Immediately west southwest of Hunga Ha'apai, a shallow water platform was formed by wave erosion of a peninsula tephra cone from the 2009 eruption[33] (Fig. 2A). The southern part of the summit caldera was characterised by a broad shallow shoal (<10 m), with crashing waves on lavas emergent at low tide, and cones associated with the 1988 eruption lying further south (Fig. 2A).

The 15 January 2022 eruption generated extreme morphological changes at Hunga, with the formation of a ~3.5 km diameter circular basin with a flat base at ~860 m below sea level (bsl) (Fig. 2B). Sub-bottom data reveals that the caldera infill is ~150 m thick (*KOPRI, pers., comm*), indicating that the structural caldera floor lies at ~1000 m bsl, and the total vertical offset is up to ~900 m when comparing with the pre-2022 surface in the caldera centre (Figs. 2A, 2B). The inner caldera reveals landslides, with ~0.5-1 km wide headwall scarps, and run-out deposit extending ~1.6-2 km into the caldera centre (Fig. 2B), and a total volume (i.e., interpreted from bathymetric data) of ~ 0.45 km^3.

The difference map between the pre- and post-eruption bathymetric datasets shows loss of material, mainly due to four processes: caldera collapse; carving of erosive channels to the north and east; landslides on the southern and western inner caldera walls, and deep erosion on the southern volcano flank (Fig. 2C, 2D). The general shape of the volcano was little affected, and the overall area of the caldera summit of ~27 km^2 remained broadly similar (Fig. 2B).

The total volume of material displaced after the eruption was 8.9 ± 0.1 km^3, with a net volume change in the caldera rim of 7.7 ± 0.1 km^3 (Fig. 2D). The major portion of the 1.2 ± 0.1 km^3 loss outside the caldera rim mask was within collapses of the upper southern flank (Fig. 2C, 2D). Results from applying a cylindrical harmonic model (CHM) shows 6.85 ± 0.05 km^3 of volume loss within the caldera basin, with the remaining ~0.9 km^3 of material eroded

from the rim, and the northern and eastern erosive channels (Fig. 2C). The greatest vertical change occurred in the northwest of the caldera, between Hunga Ha'apai and Hunga Tonga islands (Fig. 2D).

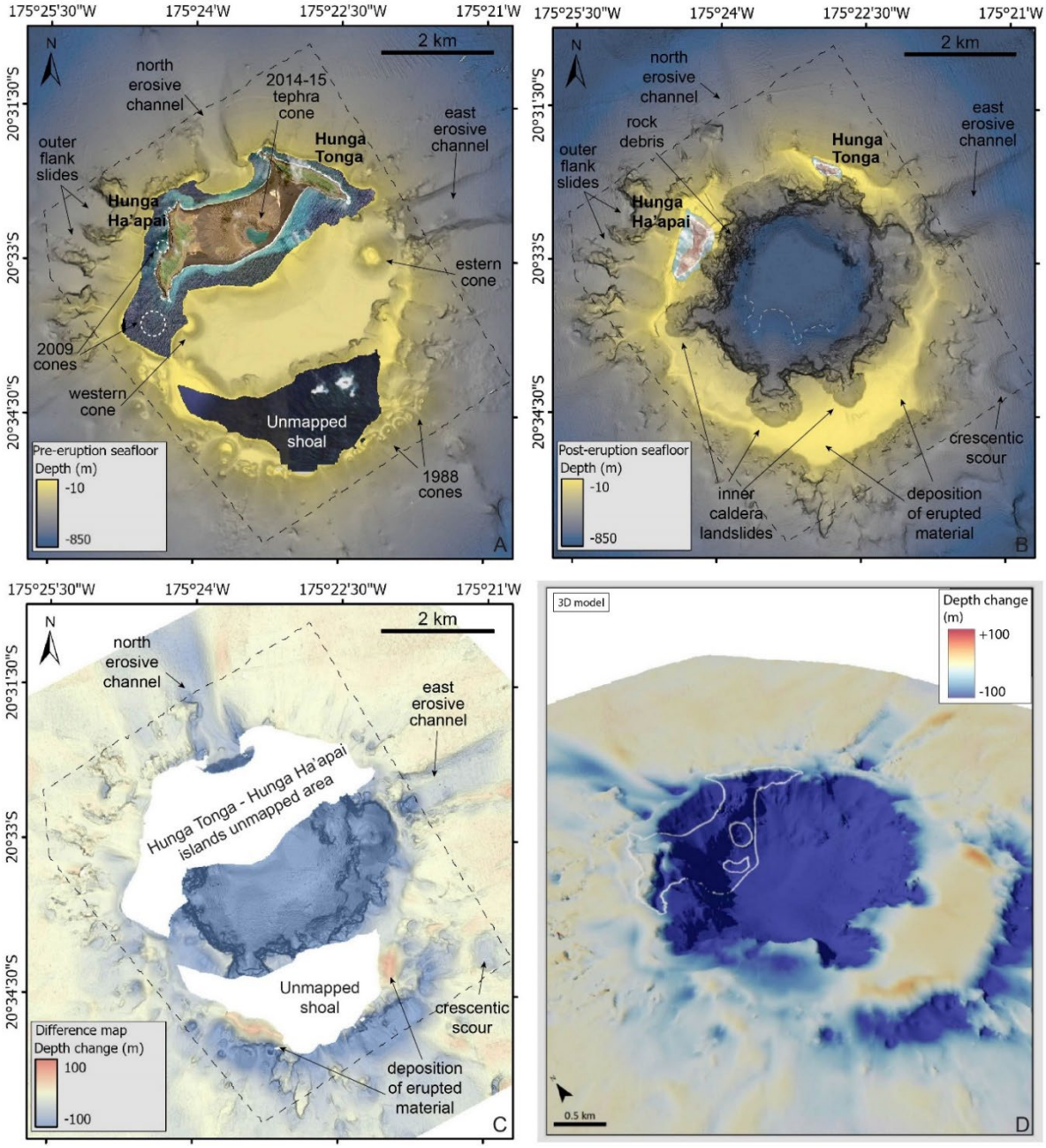


Figure 2. Bathymetric maps showing the Hunga caldera morphological evolution **(A)** pre- and **(B)** post-eruption. Black dashed line indicates post-eruption survey coverage. White circles in (A) indicate the location of the 2009 cones[33]. Grey dashed lines in (B) delimit landslide deposits characterised by rugose and variable morphology compared to the flat floor of the inner caldera. **(C)** Difference map (i.e., subtracting the 2022 bathymetric grid from the 2016 grid) and **(D)** 3D volume change model (i.e., integrating all emerged and submerged elevation models – see Methods for details). Blue colours indicate erosion, and red colours indicate deposition. White line in (D) indicates the outline of the 2014-2015 tephra cone, connecting Hunga Ha'apai and Hunga Tonga islands.

Caldera morphological features, fluid vents and water column structure

The post-eruption caldera morphology reveals caldera walls comprising concentric steep (~70° slope) and ~100 to 150 m-high escarpments, at water depths between 150 and 780 m (Fig. 3). Active fluid plumes were observed around the caldera rim in May 2022, aligned with the escarpments on the caldera wall, and the caldera rim, including several on the southeast of Hunga Ha'apai island ~50 – 130 m bsl (Fig. 3, 4). Major active vents of ~450-500 m-high were identified in two locations: a >6.9 x 10^7 m^3 vent at ~700-650 m bsl (Fig. 4) below the former position of the 2104-15 cone in the NW caldera margin, and a ~3.8 x 10^7 m^3 vent at ~650 m bsl at the SE edge of the caldera floor (Fig. 4).

Repeated transects of conductivity, temperature, and depth-pressure (CTD) vertical profiles across the Hunga caldera, collected 3-months (April 2022, *KOPRI, pers. comm.*) and 9-months (October 2022) post-eruption, revealed a 2-layer water structure within the inner caldera with a strongly marked thermocline (Fig. 5). This stratified water column shows a distinct surface water layer down to ~150-200 m water depth, with warm and low-salinity waters; and below, a deep mixed water layer with colder and denser waters, uniform to the caldera floor at ~850 m bsl (Fig. 5).

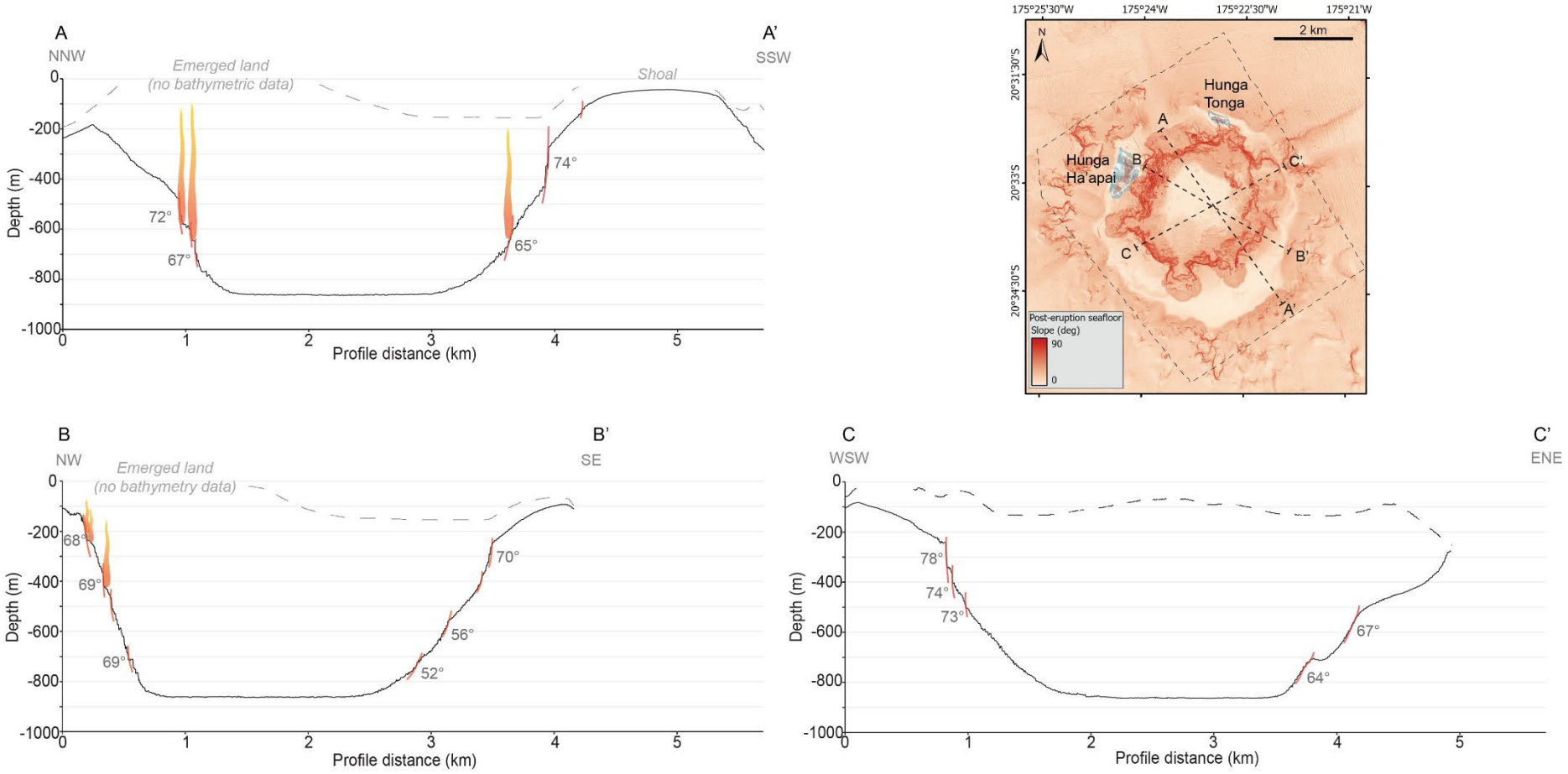


Figure 3. Bathymetric profiles (solid lines) of the Hunga caldera (dashed lines indicate the pre-eruption bathymetry). Numbers indicate the slope (in degrees). Red lines indicate interpreted ring-faults following the step-like features of the bathymetric profiles along the inner caldera wall escarpments. Graded red-to-yellow features represent the plumes identified in the echosounder during May 2022.

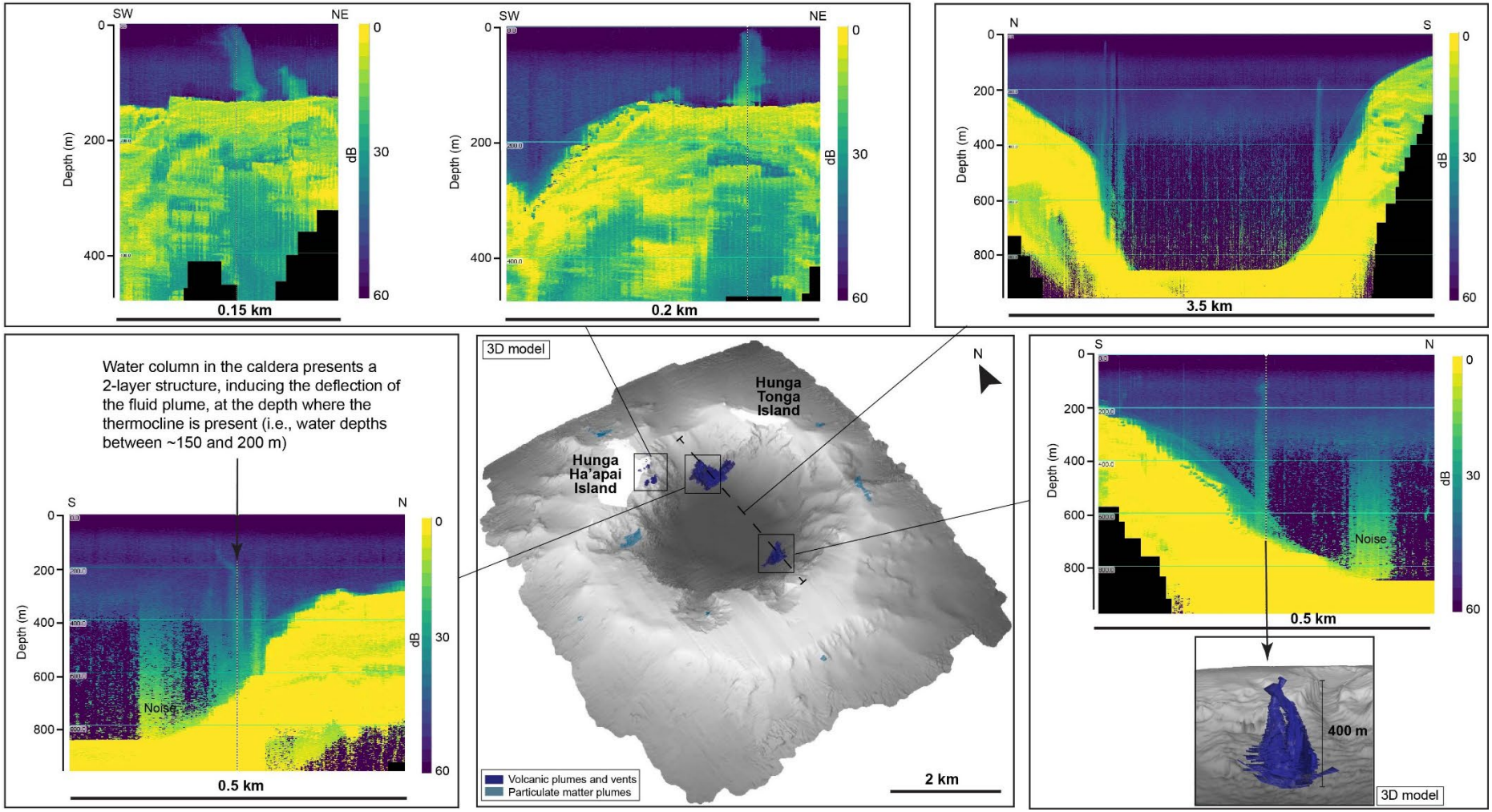


Figure 4. 3D model of Hunga volcano showing the distribution of the volcanic plumes and vents observed during the survey in May 2022, including deep volcanic vents, located at water depths between 350 and 600 m, in the south of the caldera and in the north, coinciding with the previous eruption vents (e.g., 2014-15 tephra cone, see Fig. 1, 2); and the shallow fluid plumes observed at water depths ~150 m, on the northwestern side of the caldera, south of Hunga Ha'api. 3D model and echosounder images extracted using Echoview® software.

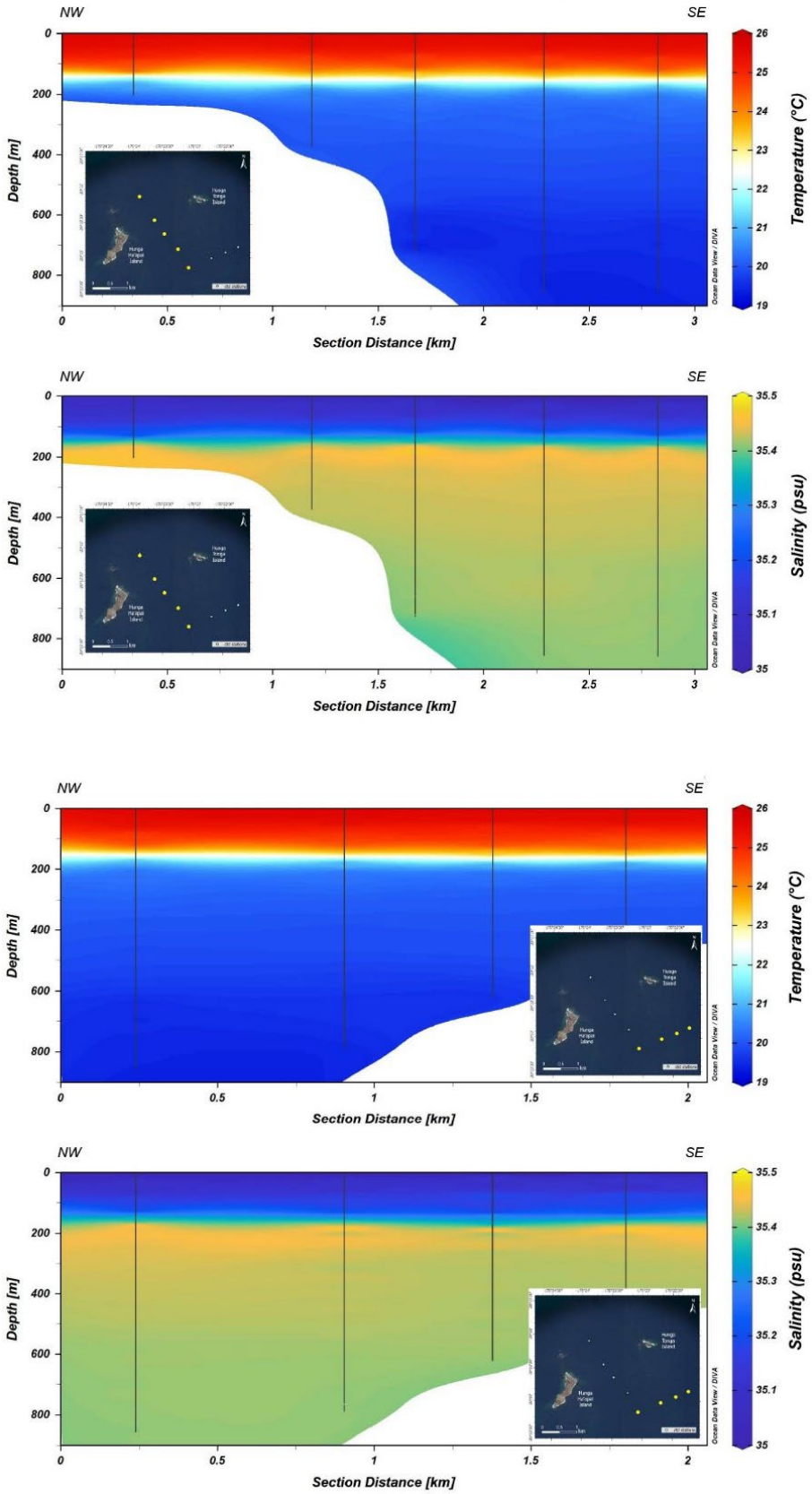


Figure 5. NW-SE (upper panels) and SW-NE (lower panels) transects showing the Temperature (°C) and Salinity (psu), used to characterise the water column structure of the inner caldera of Hunga post-2022 eruption. Green dots in insets indicate the location of the CTD vertical profiles, shown as black lines in the transects. Hydrographic transects build using OceanDataView® software (Schlitzer, R., Ocean Data View, https://odv.awi.de, 2025).

Discussion

Post-eruption activity

The two volcanic vents identified in the NW and SE caldera margins (Fig. 4) appear to mark the locations of the main eruptive vents active during the 15 January 2022 eruption. The NW area is where all activity was centred from 2014[2] up until eruptions in January 2022, while the SW site is where submarine-erupted bombs were collected in April 2022[18]. These vents were recognised four months after the eruption (May 2022) but were absent 5 months later (October 2022). This suggests that either degassing from the eruptive vents had ceased as magma withdrew, or the system was sealed by mineralisation. Earthquakes following the 2022 eruption show a progressive withdrawal of magma after the 2022 event[38]. Despite this, the shallow fluid plumes near Hunga Ha'apai (at <150 m bsl) remained active in October 2022 and May 2024 (S. Walker, *pers. comm.*), with plume heights of ~30-50 m (Fig. 4). This suggests magmatic fluid is still rising up the caldera ring fault system.

The water structure measurements indicate little vertical mixing within the caldera, suggesting strong hydrographic differences between the inner caldera and the surrounding waters, similar to the stratification seen in a (non-marine) crater lake[39]. These measurements are consistent with the uppermost ~300 m water column observations conducted in July-August 2022[40]. Our results show that water column structure remained stable for almost a year after the 2022 eruption, suggesting limited water exchange with the surrounding ocean, mainly through low points or erosive channels in the caldera rim.

Repeat bathymetric datasets from 4-months (May 2022) and 9-months (October 2022) post-eruption show no morphological changes on the landslide headwall scarps or the deposit lobes in the inner caldera (Extended Data Fig. 2). The landslide deposits are intercalated with infill caldera deposits (shown in sub-bottom seismic data, *KOPRI, pers. comm.*), interpreted as pyroclastic infill, partly burying and smoothing the surface of the landslide deposit lobes (Fig.

2). These observations collectively suggest that the caldera collapse took place during the eruption (not post-eruption), and that the landslides occurred synchronously with the collapse of the caldera. This is consistent with mechanical models of caldera ring-fault failures being initially out of equilibrium limits, so that landslides occur to reduce wall slopes[41]. With Hunga's high and steep inner-wall slopes (Fig. 3), future landslides and related tsunami cannot be dismissed for this caldera.

Caldera collapse mechanisms and eruptive volume

Calderas are a feature on volcanoes, caused by a rapid eruption of magma that drives under-pressure within a shallow reservoir, and gravitational failure of rock above[1, 42]. They typically occur when eruptions involve several cubic kilometres of magma, and they are distinct in mechanisms and dimension from explosion-excavated or pyroclastic constructed craters[43]. Based on the geomorphic analysis, the total caldera subsidence represents 6.85 ± 0.05 km^3 of magma displacement. Accounting for the estimated ~100-150 m of infill pyroclastic deposits (*KOPRI, pers. comm.*), it adds another ~0.3-0.4 km^3 approx. This suggests a total of 7.2 ± 0.05 km^3 of magma was evacuated from the upper reservoir, with likely melt density of 2.4-2.6 g/cm^3 [44] equivalent to a Dense Rock Equivalent (DRE) volume.

Ring faults develop from the magma reservoir and, propagate upward, and may later be infilled by magma and gases to accommodate volume changes inside the chamber[44]. Ring faults are rarely visible in small steep and fresh calderas, such as Hunga; but their position can be inferred from the distribution of caldera-rim cones (Fig. 2A), the step-like bathymetry of the inner caldera walls (Fig. 3), and the active venting (Fig. 3, 4). Thus, the observed caldera-rim vents and the basin structure in Hunga highlight the presence of pre-existing ring fault system, typical for small mafic calderas, where small vents are active during or between caldera-forming eruptions[45, 46]. The greatest subsidence and the steepest slopes formed in Hunga

caldera occurred on its northwestern side (Fig. 2D), i.e., where the 2014-15 and the 2021-22 eruptions occurred leading up to the main January 2022 event[44]. This and the observed post eruptive vents (Fig. 4) suggest it was the main vent area for the eruption. The presence of submarine chilled bombs consistent with compositions of the final eruption stages[18] near the southern deep gas plume (Fig. 4) indicate that this eruption vent was secondary and activated only after caldera collapse.

The bathymetric profiles of the caldera highlight distinct step slopes, especially on the southern and eastern walls (Fig. 3). These indicate progressive stepwise subsidence event or alternatively reflect structural strength contrasts during a single episode of collapse[11, 22, 41]. The contrast between the northwestern and southern and eastern walls, combined with the vent location in the north (i.e., the location where most volume is being removed from, Fig. 2D), suggests that one or more subsidence occurred with a sheer sliding failure surface in the north, with hanging walls in the south-east. This replicates a combination of trapdoor and piston-style collapses[11], or could indicate inherited structural elements from previous caldera collapse events. Moreover, at Hunga a possible incipient NE-SW rift crossing through the caldera (Fig. 1), may influence its dimensions, resulting in a similar caldera diameter before and after the 2022 eruption. This structural fabric may have also influenced the location of the main (NW) and secondary (SE) eruption vents (Fig. 4)

Collapse calderas: global overview

The morphology of calderas is controlled by the geodynamic context of their formation, including magmatic volume, composition and depth, crustal lithology and regional tectonic stress regimes[47]. Hunga erupted an andesitic composition[18], and the reservoir 2-10 km below the volcano is estimated to contain ~27 km^3 of magma[44]. When considering the caldera erupted volume of >7.2 km^3 (~26% of the reservoir) and the magma chamber roof aspect ratio (i.e.,

chamber roof thickness/width) of ~0.4, Hunga fits on the trend defined by natural collapse calderas[48]. Its overall structural caldera dimensions and volume (~5 km diameter, ~7.2 km^3 DRE), aligns with a wide range of eruptions of <10 km^3, sitting in between Pinatubo in 1991 (~2.2 km-diameter, 4.5 ± 0.8 km^3) and the Santorini Minoan eruption (~7 km-diameter, 12 ± 2 km^3)[23]. The high depth/width ratio of the Hunga caldera stands out from many global comparators[22, 23], although this may reflect is mafic composition and relatively youth, with mass-flow processes or resurgence likely to reduce it over hundreds to thousands of years.

Implications

The time-series of bathymetric maps presented here reveal outstanding geomorphological changes on Hunga volcano, highlighting syn-eruptive caldera collapse on 15 January 2022.

Our data shows that steep slopes that form along ring faults during caldera collapse generate landslides and other smaller-scale mass wasting features almost immediately (Fig. 2B). We estimated 7.2 ± 0.1 km^3 erupted from a ~27 km^3 magma reservoir, which is consistent with the caldera dimensions, and chamber roof aspect ratio of 0.4.

The 2022 eruption appear to be from a single major vent on the NW side of the caldera, causing a combination of trapdoor and piston subsidence, considering the stepped and shallower walls on the SE side of the caldera. The wide range of geomorphological changes reflect intense erosion during explosive submarine eruptions (Fig. 2D), and sudden caldera transformation caused unusual local hydrographic conditions, such as a persisting water mass which appear isolated from the surrounding ocean (Fig. 5).

Our results imply that caldera collapse during major submarine eruptions may radically transform eruption hazards, such as generating extreme density mass flows and tsunami hazards, if subsidence is rapid. In addition, fracturing and ring-fault development associated with caldera subsidence may lead to rapid and deep ingress of seawater into shallow magma

294 reservoirs, radically transforming eruption explosivity. This highlights the importance of high-
295 resolution seafloor mapping time-series and geomorphological analysis to better characterise
296 shallow submarine caldera systems in volcanic arcs throughout the world
297
298

Methods

Pre-eruption bathymetry datasets were acquired in November 2015 using a WASSP DRX-46 echosounder (160kHz) mounted on MV Pacific Rose, and in May 2016 onboard R/V Falkor (FK160407) using a Kongsberg-Maritime EM302 (30kHz) echosounder. The repeat post-eruption swath bathymetry of Hunga and surroundings is a mosaic of different datasets acquired during several surveys, including: *i)* April 2022, by R/V Araon, using a Kongsberg EM120 (12kHz) multibeam echosounder (summit and surrounding flanks); *ii)* May 2022, on M/V Pacific Horizon, using a WASSP DRX-46 (80kHz) echosounder (summit plateau and upper flanks); *iii)* April-May 2022, by R/V Tangaroa, using a Kongsberg EM302 (30kHz) multibeam echosounder (surrounding flanks)[20, 49]; *iv)* July-September 2022, using the SEA-KIT International's Uncrewed Surface Vessel (USV) *Maxlimer*, with a Kongsberg EM710 (70-100 kHz) multibeam echosounder system (summit area)[50]; and *v)* October 2022, on M/V Pacific Dawn, using a WASSP DRX-46 (80 kHz) echosounder (summit area).

All bathymetric datasets were corrected for heading, depth, pitch, heave and roll. The post processing was conducted using QPS Qimera software (V 2.3.5), and all processed multibeam datasets were gridded at a 10-m horizontal resolution. Corrections for sound velocity were made using direct measurements during survey and from sound velocity profiles calculated from conductivity-temperature-depth (CTD) vertical profiles.

CTD profiles collected in the October 2022 survey were acquired using a *Ruskin RBR* logger with a sampling rate of 2 Hz. Conductivity data was used to calculate salinity, and depth was calculated from the data recorded by the pressure sensor. Data recorded were exported directly to OceanDataView® software, used to represent the water column structure and hydrographic parameters along the two transects of CTD profiles collected in the caldera.

Water column anomalies were systematically detected from the echosounder data from the surveys conducted in May and October 2022, and Echoview® software was used for sonar

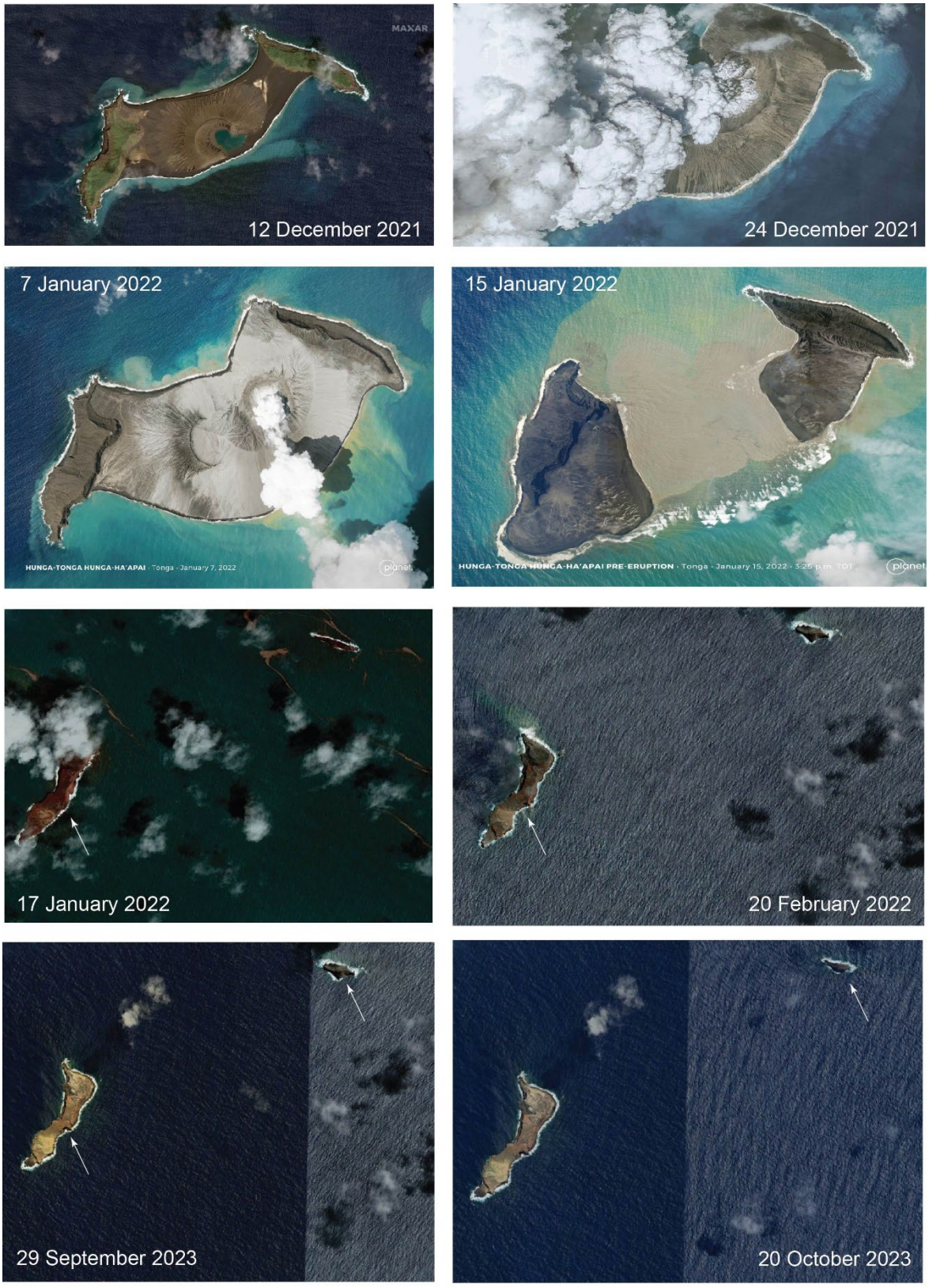
reanalysis to identify and map seafloor vents emitting gas fluids and/or particles. Positions of seafloor vents off the direct navigational track were estimated by their relative detection in vertical and laterally angled beams of each multibeam track and triangulated between parallel survey lines. Disturbance height and vent size were estimated by the strongest beam response (closest to the vent). Errors in position are estimated to be ~20 m in X and Y, while vents height uncertainties are ~30 m depending on the position of the vent in relation to the sensor and the observed margin of water disturbance.

The subaerial (emergent) topography of the Hunga system has been documented since 2015, with increased focus from late 2021 to present, using Maxar WorldView (WV-2, WV-3 stereo imaging at 0.5 m/pixel resolution). Digital Elevation Models (DEM) generated at 1-m Ground Scale Distance (GSD) were calibrated and validated by NASA ICESat-2 lidar altimetry tracks, based on footprints with absolute ranging precision (and hence COM referenced) at < 20 cm. The DEM were complemented by field differential GPS surveys in 2018 and 2019 on visits to the 2014/15 tephra cone (*Fig. 1B, 2A*) by SSV Seamans and students from the Sea Education Association (SEA) program assisted by NASA colleagues. Integrated CSA Radarsat Constellation Mission spotlight SAR images every 2-3 days were acquired from December 2021 through April 2022 using multiple beam geometries at ~ 1-m spatial sampling, courtesy the RCM vetter user program. These satellite data were further used to track the volumetric changes at Hunga Ha'apai and Hunga Tonga islands from late January 2015 to present, with subaerial topography (including a drone-based, RTK-GPS controlled survey carried out in November 2015 by the University of Auckland), merged with the various bathymetric datasets.

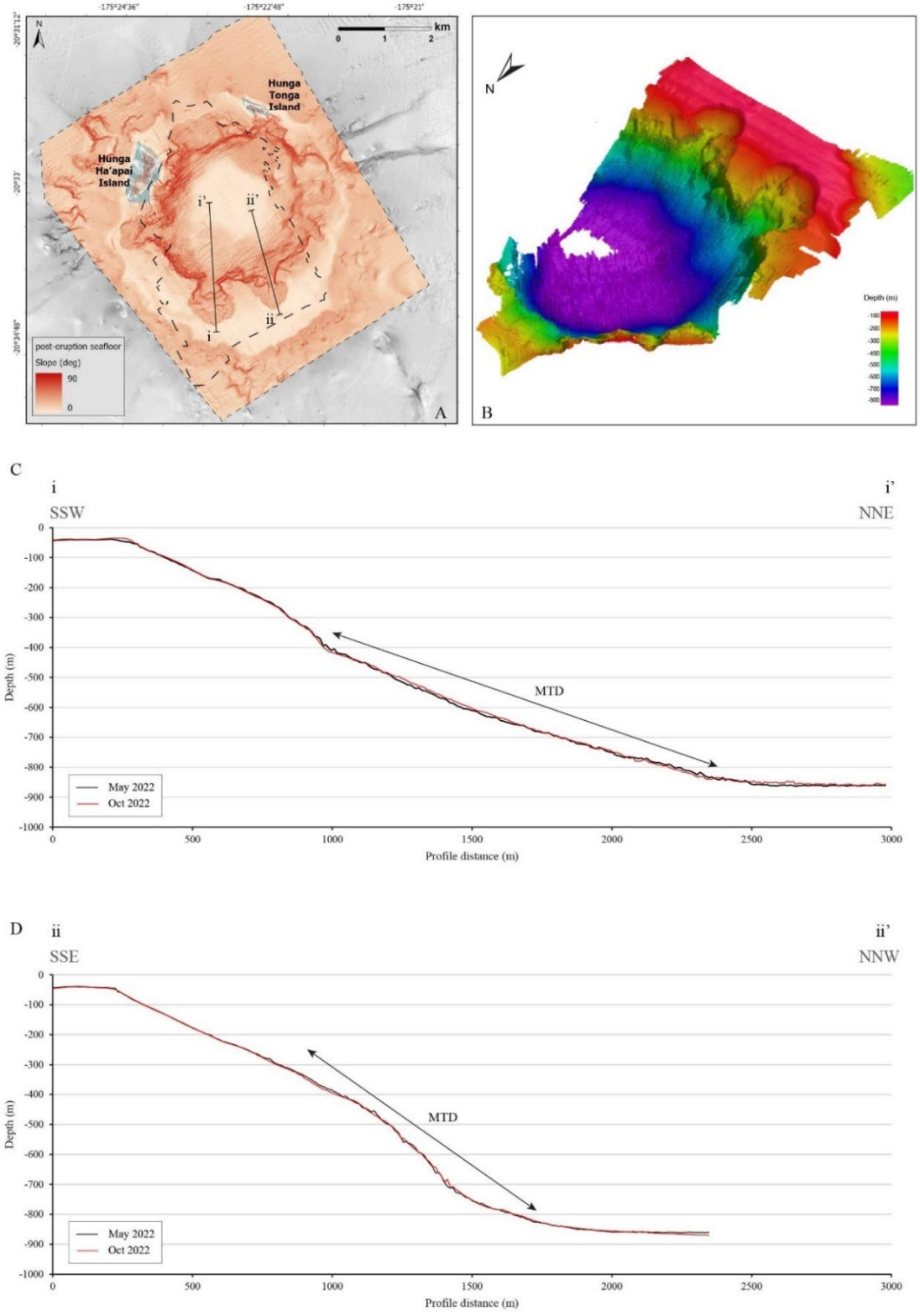
Integrated 3D topographic models combining the pre- and post-eruption sonar bathymetry were used to construct a 10-m DEM of the entire Hunga edifice. This was used as a baseline to measure differential volumes after careful co-registration and levelling against the regional seafloor "ground plane" as a stable reference over this time of period. A cylindrical harmonic

model (CHM) approach was applied to model a set of best fitting cylindrical harmonic coefficients and a power spectrum that rendered ~95% of the three-dimensional shape of the Hunga caldera. This produced between 10 to 12 values, which were integrated to produce volume estimates to compare with those measured from the differential sonar/Satellite DEM datasets with agreement to a few percent. The CHM approach provides validation and calibration of the displaced volume. A similar approach was carried out to evaluate the volume of the 2014-2015 Hunga tephra cone[36]. Drone-based (DJI Phantom 4) photogrammetry of Hunga Ha'apai and Hunga Tonga islands was collected during surveys conducted in May and October 2022. These aerial photogrammetry datasets were used to estimate changes in the subaerial expression of the system via Structure-from-Motion (SfM) computations (i.e., developed at NASA for planetary spaceflight).

Extended data



Extended Data Fig. 1. Satellite images showing the emergent parts of Hunga caldera, Hunga Ha'apai and Hunga Tonga islands, undergoing continuous changes since December 2021 (upper panels) to October 2023 (lower right panel). White arrows in the lower panels indicate the erosion of Hunga Ha'apai and Hunga Tonga. Satellite imagery sources: Maxar Technologies and Google Earth.



Extended Data Fig. 2. (A) Slope map of Hunga caldera, calculated from the post-eruption bathymetric dataset. Black dashed line indicates the coverage of the repeated seafloor mapping survey conducted in October 2022. **(B)** 3D image of the repeated bathymetric dataset, showing the detail of the two submarine landslides of the southern rim of the Hunga caldera. **(C)** and **(D)** Comparison of the bathymetric profiles of the submarine landslides, 4-month (May2022, black line) and 9-month (October 2022, red line) post-eruption, indicating the location of the landslide Mass Transport Deposits (MTD).

References

1. Acocella V, Funiciello R, Marotta E, Orsi G, de Vita S. The role of extensional structures on experimental calderas and resurgence. *Journal of Volcanology and Geothermal Research* 2004, **129**(1-3)**:** 199-217.

2. Brenna M, Cronin SJ, Smith IEM, Pontesilli A, Tost M, Barker S*, et al.* Post-caldera volcanism reveals shallow priming of an intra-ocean arc andesitic caldera: Hunga volcano, Tonga, SW Pacific. *Lithos* 2022, **412-413**.

3. Madden-Nadeau A, Cassidy M, Pyle D, Mather T, Watt S, Engwell S*, et al.* The magmatic and eruptive evolution of the 1883 caldera-forming eruption of Krakatau: Integrating field-to crystal-scale observations. *Journal of Volcanology and Geothermal Research* 2021, **411:** 107176.

4. Borrero JC, Cronin SJ, Latu'ila FH, Tukuafu P, Heni N, Tupou AM*, et al.* Tsunami Runup and Inundation in Tonga from the January 2022 Eruption of Hunga Volcano. *Pure Appl Geophys* 2023, **180**(1)**:** 1-22.

5. Pallister JS, Schneider DJ, Griswold JP, Keeler RH, Burton WC, Noyles C*, et al.* Merapi 2010 eruption—Chronology and extrusion rates monitored with satellite radar and used in eruption forecasting. *Journal of Volcanology and Geothermal Research* 2013, **261:** 144-152.

6. Procter J, Cronin SJ, Fuller IC, Lube G, Manville V. Quantifying the geomorphic impacts of a lake-breakout lahar, Mount Ruapehu, New Zealand. *Geology* 2010, **38**(1)**:** 67-70.

7. Waythomas CF, Scott WE, Nye CJ. The Geomorphology of an Aleutian Volcano following a Major Eruption: the 7–8 August 2008 Eruption of Kasatochi Volcano, Alaska, and Its Aftermath. *Arctic, Antarctic, and Alpine Research* 2010, **42**(3)**:** 260-275.

8. Allen RW, Berry C, Henstock TJ, Collier JS, Dondin FJY, Rietbrock A*, et al.* 30 Years in the Life of an Active Submarine Volcano: A Time-Lapse Bathymetry Study of the Kick-'em-Jenny Volcano, Lesser Antilles. *Geochemistry, Geophysics, Geosystems* 2018, **19**(3)**:** 715-731.

9. Caress DW, Clague DA, Paduan JB, Martin JF, Dreyer BM, Chadwick WW*, et al.* Repeat bathymetric surveys at 1-metre resolution of lava flows erupted at Axial Seamount in April 2011. *Nature Geoscience* 2012, **5**(7)**:** 483-488.

10. Ikegami F, McPhie J, Carey R, Mundana R, Soule A, Jutzeler M. The Eruption of Submarine Rhyolite Lavas and Domes in the Deep Ocean – Havre 2012, Kermadec Arc. *Frontiers in Earth Science* 2018, **6**.

11. Sanjo R, Sugai T. The spatiotemporal development of downsag and trapdoor structures during caldera subsidence with 1–10 km in diameter in analogue sandbox experiments. *Journal of Volcanology and Geothermal Research* 2025, **461:** 108294.

12. Paris R. Source mechanisms of volcanic tsunamis. *Philos Trans A Math Phys Eng Sci* 2015, **373**(2053).

13. Poli P, Shapiro NM. Rapid Characterization of Large Volcanic Eruptions: Measuring the Impulse of the Hunga Tonga Ha'apai Explosion From Teleseismic Waves. *Geophysical Research Letters* 2022, **49**(8).

14. Purkis SJ, Ward SN, Fitzpatrick NM, Garvin JB, Slayback D, Cronin SJ*, et al.* The 2022 Hunga-Tonga megatsunami: Near-field simulation of a once-in-a-century event. *Science advances* 2023, **9**(15)**:** eadf5493.

15. Matoza RS, Fee D, Assink JD, Iezzi AM, Green DN, Kim K*, et al.* Atmospheric waves and global seismoacoustic observations of the January 2022 Hunga eruption, Tonga. *Science* 2022, **377**(6601)**:** 95-100.

16. Van Eaton AR, Lapierre J, Behnke SA, Vagasky C, Schultz CJ, Pavolonis M*, et al.* Lightning Rings and Gravity Waves: Insights Into the Giant Eruption Plume From Tonga's Hunga Volcano on 15 January 2022. *Geophysical Research Letters* 2023, **50**(12).

17. Mastin LG, Van Eaton AR, Cronin SJ. Did steam boost the height and growth rate of the giant Hunga eruption plume? *Bulletin of Volcanology* 2024, **86**(7)**:** 64.

18. Wu J, Cronin SJ, Brenna M, Park S-H, Pontesilli A, Ukstins IA*, et al.* Low sulfur emissions from 2022 Hunga eruption due to seawater–magma interactions. *Nature Geoscience* 2025, **18**(6)**:** 518-524.

19. Vömel H, Evan S, Tully M. Water vapor injection into the stratosphere by Hunga Tonga-Hunga Ha'apai. *Science* 2022, **377**(6613)**:** 1444-1447.

20. Seabrook S, Mackay K, Watson SJ, Clare MA, Hunt JE, Yeo IA*, et al.* Volcaniclastic density currents explain widespread and diverse seafloor impacts of the 2022 Hunga Volcano eruption. *Nat Commun* 2023, **14**(1)**:** 7881.

21. Clare MA, Yeo IA, Watson S, Wysoczanski R, Seabrook S, Mackay K*, et al.* Fast and destructive density currents created by ocean-entering volcanic eruptions. *Science* 2023, **381**(6662).

22. Acocella V. Understanding caldera structure and development: An overview of analogue models compared to natural calderas. *Earth-Science Reviews* 2007, **85**(3-4)**:** 125-160.

23. Geshi N, Ruch J, Acocella V. Evaluating volumes for magma chambers and magma withdrawn for caldera collapse. *Earth and Planetary Science Letters* 2014, **396:** 107-115.

24. White JDL, Smellie JL, Clague DA. Introduction: A Deductive Outline and Topical Overview of Subaqueous Explosive Volcanism. *Explosive Subaqueous Volcanism*, 2003, pp 1-23.

25. Kano K. Subaqueous Pumice Eruptions and Their Products: A Review. *Explosive Subaqueous Volcanism*, 2003, pp 213-229.

26. Yuasa M, Kano K. Submarine Silicic Calderas on the Northern Shichito-Iwojima Ridge, Izu-Ogasawara (Bonin) Arc, Western Pacific. *Explosive Subaqueous Volcanism*, 2003, pp 231-243.

27. Smith IEM, Price RC. The Tonga–Kermadec arc and Havre–Lau back-arc system: Their role in the development of tectonic and magmatic models for the western Pacific. *Journal of Volcanology and Geothermal Research* 2006, **156**(3-4)**:** 315-331.

28. Wright IC. Nature and tectonic setting of the southern Kermadec submarine arc volcanoes: An overview. *Marine Geology* 1994, **118:** 217-236.

29. Bevis M, Taylor FW, Schutz BE, Recy J, Isacks BL, Helu S*, et al.* Geodetic observations of very rapid convergence and back-arc extension at the Tonga arc. *Nature* 1995, **374**(6519)**:** 249-251.

30. Bryan W, Stice G, Ewart A. Geology, petrography, and geochemistry of the volcanic islands of Tonga. *Journal of geophysical research* 1972, **77**(8)**:** 1566-1585.

31. Nappi G, Renzully A, Falsaperla S. Annual report of The World Volcanic Eruptions in 1988. Bull. Volcanic Eruptions; 1988.

32. Siebert L, Simkin T, Kimberly P. *Volcanoes of the World*. Univ of California Press, 2011.

33. Bohnenstiehl DR, Dziak RP, Matsumoto H, Lau TKA. Underwater acoustic records from the March 2009 eruption of Hunga Ha'apai-Hunga Tonga volcano in the Kingdom of Tonga. *Journal of Volcanology and Geothermal Research* 2013, **249:** 12-24.

34. Vaughan RG, Webley PW. Satellite observations of a surtseyan eruption: Hunga Ha'apai, Tonga. *Journal of Volcanology and Geothermal Research* 2010, **198**(1-2)**:** 177-186.

35. Cronin SJ, Brenna M, Smith IEMS, Barker SJ, Tost M, Ford M*, et al.* New Volcanic Island Unveils Explosive Past. *EOS* 2017.

36. Garvin JB, Slayback DA, Ferrini V, Frawley J, Giguere C, Asrar GR, Andersen K. Monitoring and Modeling the Rapid Evolution of Earth's Newest Volcanic Island: Hunga Tonga Hunga Ha'apai (Tonga) Using High Spatial Resolution Satellite Observations. *Geophys Res Lett* 2018, **45**(8)**:** 3445-3452.

37. Caulfield JT, Cronin SJ, Turner SP, Cooper LB. Mafic Plinian volcanism and ignimbrite emplacement at Tofua volcano, Tonga. *Bulletin of Volcanology* 2011, **73**(9)**:** 1259-1277.

38. Liu Y, Zhou P, Zhang F, Lin J, Zhang J, Zhang X*, et al.* Physical Mechanisms of Volcanic Earthquakes After the 2022 Hunga Eruption, Tonga. *Terra Nova* 2025, **37**(5)**:** 297-303.

39. Christopoulou ME, Mertzimekis TJ, Nomikou P, Papanikolaou D, Carey S, Mandalakis M. Influence of hydrothermal venting on water column properties in the crater of the Kolumbo submarine volcano, Santorini volcanic field (Greece). *Geo-Marine Letters* 2016, **36**(1)**:** 15-24.

40. Walker SL, de Ronde CEJ. Ongoing Activity at Hunga Submarine Volcano, Tonga: The Case for Better Monitoring of Submarine Volcanoes Worldwide. *Geochemistry, Geophysics, Geosystems* 2024, **25**(8).

41. Harnett CE, Watson RA, Holohan EP, Schöpfer MPJ. Collapse caldera walls: Mechanical controls on slope failure and morphology. *Journal of Volcanology and Geothermal Research* 2023, **442**.

42. Geyer A, Martí- J. A short review of our current understanding of the development of ring faults during collapse caldera formation. *Frontiers in Earth Science* 2014, **2**.

43. Lipman PW. Subsidence of ash-flow calderas: relation to caldera size and magma-chamber geometry. *Bulletin of Volcanology* 1997, **59**(3)**:** 198-218.

44. Le Mével H, Miller CA, Ribó M, Cronin S, Kula T. The magmatic system under Hunga volcano before and after the 15 January 2022 eruption. *Science Advances* 2023, **9**(50)**:** eadh3156.

45. Walter TR, Troll VR. Formation of caldera periphery faults: an experimental study. *Bulletin of Volcanology* 2001, **63:** 191-203.

46. Munro DC, Rowland SK. Caldera morphology in the western Galapagos and implications for volcano eruptive behaviour and mechanisms of caldera formation. *Journal of Volcanology and Geothermal Research* 1996, **72:** 85-100.

47. Sobradelo R, Geyer A, Martí J. Statistical data analysis of the CCDB (Collapse Caldera Database): Insights on the formation of caldera systems. *Journal of Volcanology and Geothermal Research* 2010, **198**(1-2)**:** 241-252.

48. Geyer A, Folch A, Martí J. Relationship between caldera collapse and magma chamber withdrawal: An experimental approach. *Journal of Volcanology and Geothermal Research* 2006, **157**(4)**:** 375-386.

49. Mackay K, Clark MR, Seabrook S, Armstrong E, Barr N, Frontin-Rollet G*, et al.* Environmental impacts of the 2022 eruption of Hunga Tonga-Hunga Ha'apai: voyage report of part 1 of the TesMAP survey of the region in April-May 2022 (TAN2206); 2022.

50. NIWA-NipponFoundation. NIWA-Nippon Foundation Tonga Eruption Seabed Mapping Project (TESMaP). Digital elevation models of Hunga volcano, Tonga, from the MAX2201 voyage, July–August 2022. Zenodo; 2023.